Title: Modified Gravity, Gravitational Waves and Black Holes

Date: Mar 16, 2017 11:00 AM

URL: http://pirsa.org/17030021

Abstract: <span style="font-size:12.0pt;font-family:"Times New Roman",serif;
mso-fareast-font-family:Calibri;mso-fareast-theme-font:minor-latin;mso-ansi-language:
EN-CA;mso-fareast-language:EN-CA;mso-bidi-language:AR-SA">Modified gravitation known as Scalar-Tensor- Vector-Gravity (STVG) and MOG and its consequences for dark matter and dark energy in astrophysics and cosmology and black holes is reviewed. A variable speed of light (VSL) cosmology is compared to inflation. MOG predictions for gravitational waves are compared to the LIGO/Virgo collaboration data. MOG â€“ black hole predictions for the sizes of the Sagittarius A* shadow are compared to the sizes predicted by the Schwarzschild and Kerr solutions. A possible void cosmology is compared to the standard cosmology based on dark energy and the cosmological constant.

Contents

1. Introduction

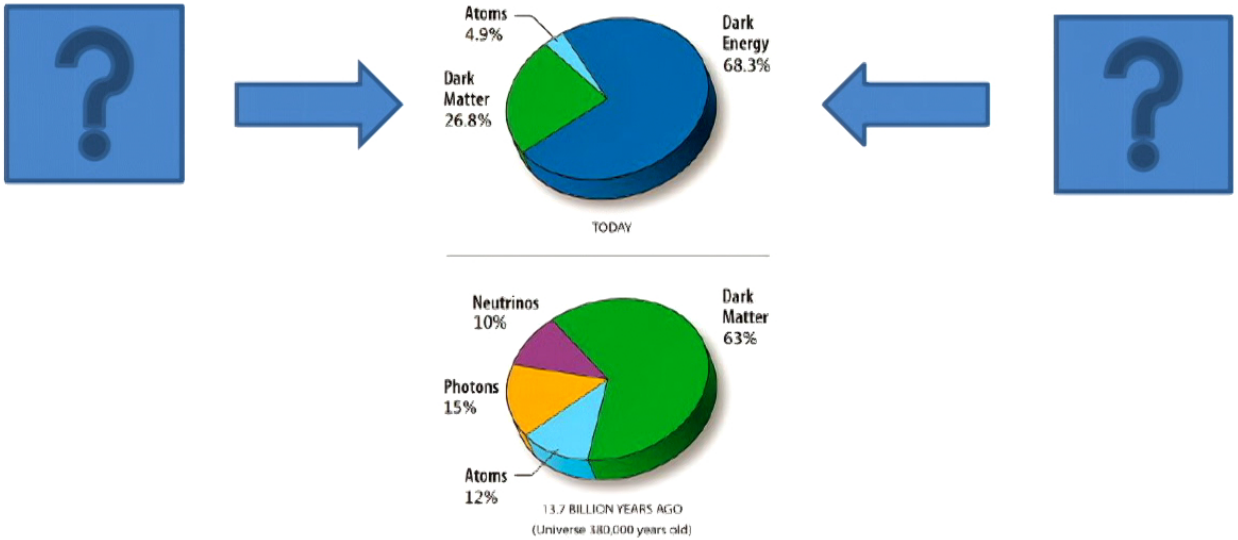

- Observations of the dynamics of galaxies as well as the dynamics of the whole Universe reveal that a main part of the Universe's mass must be missing -- dark matter. The universe undergoes an accelerated expansion -- dark energy.

- Observations of galaxies reveal that there is a discrepancy between the observed rotational velocities and the mass inferred from luminous matter (Rubin, Thonnard & Ford 1978, Astroph. J. 225, L107 (1978)).

- An alternative approach to the problem of missing mass is to replace dark matter by a modified gravity theory. The generally covariant Modified Gravity (MOG) theory is a Scalar-Tensor-Vector Gravity theory (STVG, JWM, JCAP, 0603 004 (2006), arXiv:0506021 [gr-qc]).

- To-date no convincing detection of dark matter particles has been achieved in either laboratory or satellite experiments.

- The LUX experimental data from the Sanford Underground Research Facility (Lead, South Dakota) using a 370 kg liquid Xenon detector has ruled out low-mass WIMPs, and set new bounds on elastic scattering cross sections of WIMPs. No WIMP signals were detected in the LUX or Chinese PANDAX (1/2 ton Xenon) experiments.

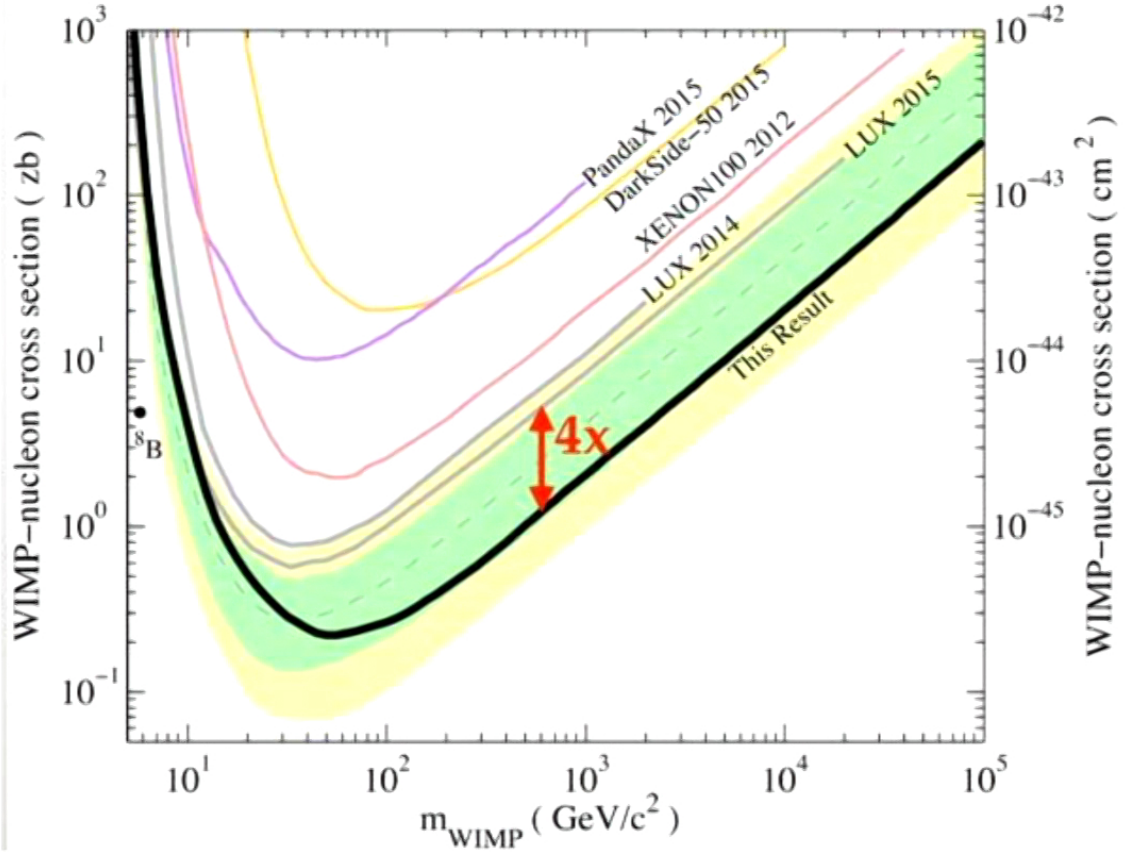

https://angel.co/mog

Experimental data that must be explained and fitted by MOG:

1. Planck and WMAP cosmic microwave background (CMB) data:
   Structure growth producing stars and galaxies.
   The CMB angular acoustical power spectrum.
   Matter power spectrum.
   Accelerated expansion of the universe and dark energy

2. Galaxy rotation curves and galaxy evolution and stability.
3. Galactic cluster dynamics.

4. Bullet Cluster 1E0657-558 and Abell 520 cluster "train wreck" collision.

5. Gravitational lensing.
6. Binary pulsar timing (PSR 1913+16 – Hulse-Taylor binary pulsar and other pulsars).

7. Solar system experiments:
   Weak equivalence experiments, light deflection by Sun, Shapiro time delay (Cassini probe), planetary orbits.

8. Strong gravity: LIGO gravitational wave detection. Event Horizon Telescope black hole observations.

2. MOG Field Equations (JCAP 0603 004 (2006), arXiv:gr-qc/0506021)

- The MOG action is given by

$$S = S_G + S_{\phi_\mu} + S_S + S_M$$

where

$$S_G = \frac{1}{16\pi}\int d^4x\sqrt{-g}\left[\frac{1}{G}(R+2\Lambda)\right]$$

$$S_{\phi_\mu} = -\int d^4x\sqrt{-g}\left[\frac{1}{4}B^{\mu\nu}B_{\mu\nu} - V(\phi_\mu)\right]$$

$$S_S = \int d^4x\sqrt{-g}\left[\frac{1}{G^3}\left(\frac{1}{2}g^{\mu\nu}\partial_\mu G\partial_\nu G - V(G)\right) + \frac{1}{\mu^2 G}\left(\frac{1}{2}g^{\mu\nu}\partial_\mu\mu\partial_\nu\mu - V(\mu)\right)\right]$$

$$B_{\mu\nu} = \partial_\mu\phi_\nu - \partial_\nu\phi_\mu$$

S_M denotes the matter field action.

- The MOG field equations:

$$G_{\mu\nu} - g_{\mu\nu}\Lambda + Q_{\mu\nu} = -8\pi G T_{\mu\nu}$$

$$\frac{1}{\sqrt{-g}}\partial_\nu(\sqrt{-g}B^{\mu\nu}) + \mu^2\phi^\mu = -J^\mu$$

$$\partial_\sigma B_{\mu\nu} + \partial_\mu B_{\nu\sigma} + \partial_\nu B_{\sigma\mu} = 0$$

$$\nabla_\alpha\partial^\alpha G + V'(G) + N(G) + \frac{G}{16\pi}(R + 2\Lambda) = 0 \quad \nabla_\alpha\partial^\alpha\mu + V'(\mu) + P(\mu) = 0$$

$$Q_{\mu\nu} = \frac{2}{G^2}(\nabla^\alpha G\nabla_\alpha G g_{\mu\nu} - \nabla_\mu G\nabla_\nu G) - \frac{1}{G}(\Box G g_{\mu\nu} - \nabla_\mu\nabla_\nu G).$$

$$T_{\mu\nu} = T^M_{\mu\nu} + T^\phi_{\mu\nu} + T^G_{\mu\nu} + T^\mu_{\mu\nu} \qquad J^\mu = \kappa T^{M\mu\nu}u_\nu \quad G = G_N(1+\alpha)$$

$$T^{M\mu\nu} = (\rho_M + p_M)u^\mu u^\nu - p_M g^{\mu\nu} \quad J^\mu = \kappa\rho_M u^\mu \quad u^\nu u_\nu = 1$$

$$V(\phi_\mu) = -\frac{1}{2}\mu^2\phi^\mu\phi_\mu \qquad Q = \int d^3x J^0 = \kappa M = \sqrt{\alpha G_N}M$$

- The action for a test particle is

$$S_{\rm tp} = -\left(m \int ds + q \int \phi_\mu u^\mu ds \right) \quad q = \kappa m = \sqrt{\alpha G_N} m$$

- For the weak spherically symmetric field solution (Q > 0):

$$\phi_0(r) = -Q \frac{\exp(-\mu r)}{r} \qquad Q = \kappa M = \sqrt{\alpha G_N} M$$

- Test particle equation of motion:

$$\frac{du^\mu}{ds} + \Gamma^\mu{}_{\alpha\beta} u^\alpha u^\beta = \frac{q}{m} B^\mu{}_\nu u^\nu \qquad \frac{d^2 r}{dt^2} + \frac{GM}{r^2} = \frac{qQ}{m} \frac{\exp(-\mu r)}{r^2} (1 + \mu r)$$

$$\frac{q}{m} = \kappa = \sqrt{\alpha G_N} \quad qQ/m = \kappa^2 M = \alpha G_N M \text{ and } G = G_N(1+\alpha)$$

- The equation of motion and the modified acceleration law satisfy the (weak) equivalence principle:

$$a(r) = -\frac{G_N M}{r^2} \left[1 + \alpha - \alpha \exp(-r/r_0) \left(1 + \frac{r}{r_0} \right) \right] \quad r_0 = 1/\mu$$

- The modified weak field Newtonian potential is given by

$$\Phi(r) = -\frac{G_N M}{r}\left[1 + \alpha - \alpha e^{-\mu r}\right]$$

- For an extended distribution of matter:

$$\nabla^2\Phi(\mathbf{r}) = 4\pi G_N \rho(\mathbf{r}) + \alpha\mu^2 G_N \int \frac{e^{-\mu|\mathbf{r}-\tilde{\mathbf{r}}|}}{|\mathbf{r}-\tilde{\mathbf{r}}|}\rho(\tilde{\mathbf{r}})\; d^3\tilde{\mathbf{r}}$$

- A photon follows a null-geodesic path:

$$k^\mu \nabla_\mu k^\nu = 0 \qquad \frac{dk^\mu}{d\lambda} + \Gamma^\mu{}_{\alpha\beta} k^\alpha k^\beta = 0$$

k^μ = photon momentum

- The gravitational degrees of freedom in MOG:

$g_{\mu\nu}$: spin-2 massless graviton

ϕ_μ : spin-1 massive "graviton"

G : spin-0 massless "graviton"

- MOG is a purely gravitational theory. It is generally covariant and satisfies the weak equivalence principle. Particles are in free-fall independent of their composition but they do not move along geodesics. This can be tested by experiment.

Static spherically symmetric MOG solution of G = G_N(1 + α) for weak gravity:

$$\Box G + N(G) - \frac{\partial V(G)}{\partial G} = -\frac{GR}{16\pi} \qquad \Box G = \nabla_\alpha \partial^\alpha G$$

$$\alpha''(r) + \frac{2}{r}\alpha'(r) = -\frac{\partial V(\alpha)}{\partial \alpha}$$

$$G = G_N(1+\alpha) \quad G_N = 1 \quad \alpha(r) = A\arctan(r)$$

$$V(\alpha(r)) = \frac{3}{4}\cos(2\alpha(r)) + \frac{1}{16}\cos(4\alpha(r)) + 2\ln(\sin(\alpha(r))) + C$$

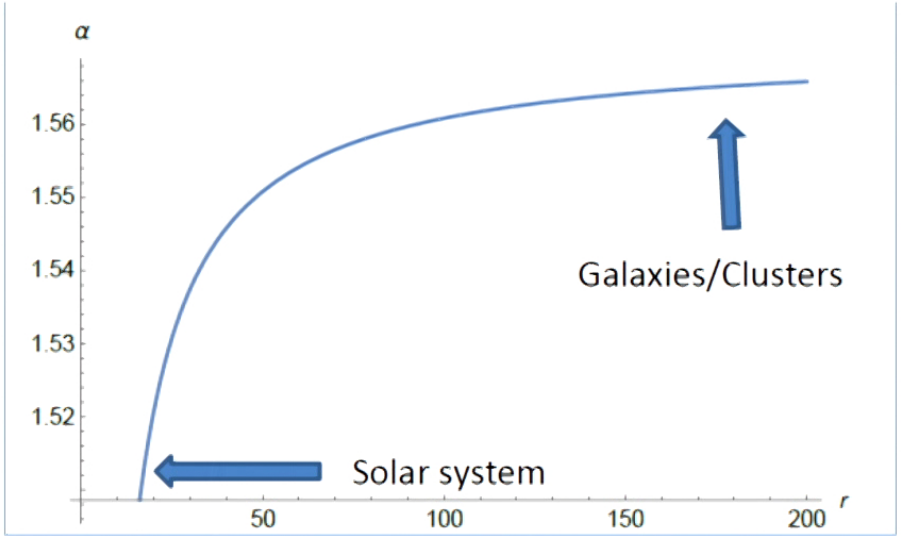

3. Rotation Curves of Galaxies (JWM and S. Rahvar, MNRAS 436, 1439 (2013), arXiv:1306.6385 [astro-ph])

- We adopt the best-fitting values:

$$\alpha = 8.89 \pm 0.34 \qquad \mu = 0.042 \pm 0.004\,\mathrm{kpc}^{-1}$$

We let the mass-to-light ratio M/L be the only free parameter, and obtain fits to the Ursa Major catalogue of galaxies.

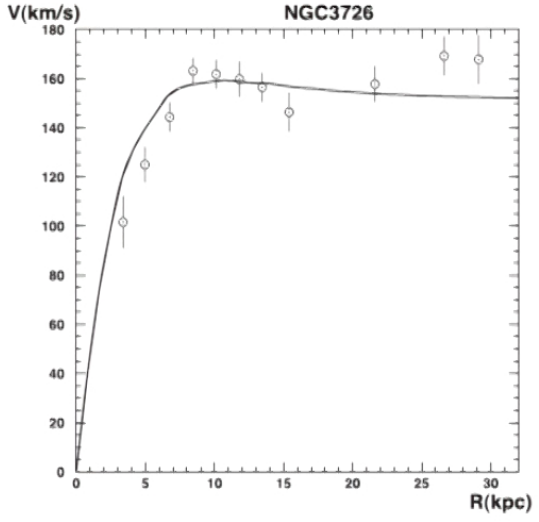

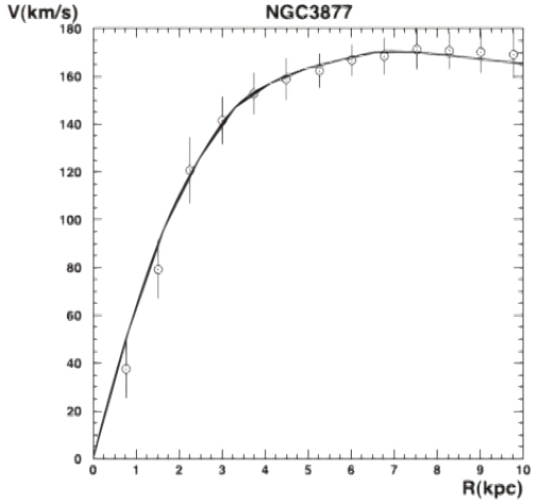

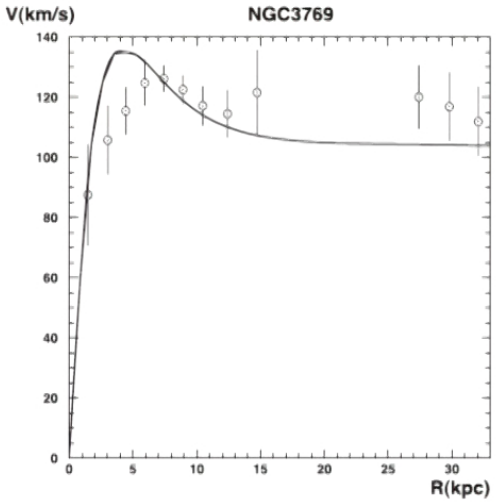
V(km/s)
NGC3769
R(kpc)

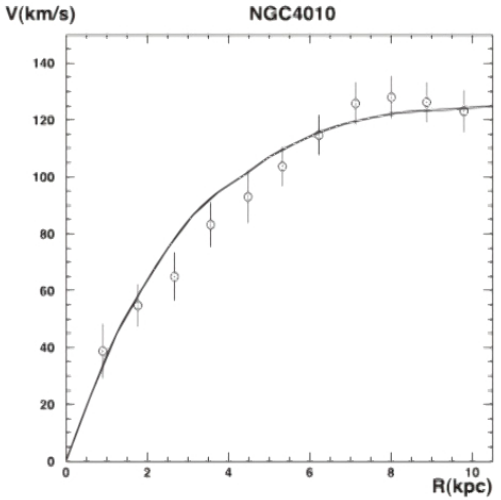
V(km/s)
NGC4010
R(kpc)

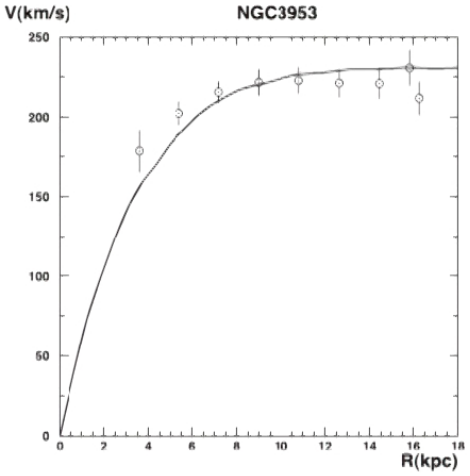
V(km/s)
NGC3953
R(kpc)

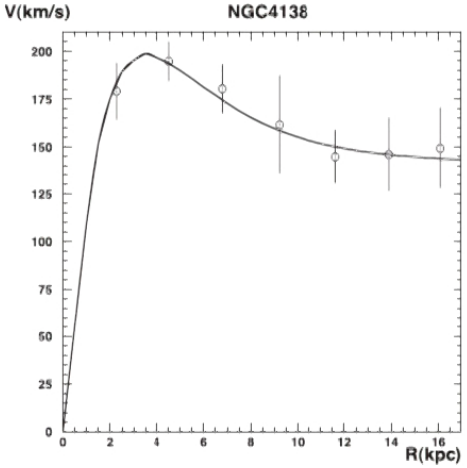
V(km/s)
NGC4138
R(kpc)

15

MOG Fit To Milky Way Galaxy

JWM and V. T. Toth, Phys. Rev. D91, 043004 (2015), arXiv:1411.6701 [astro-ph.GA]

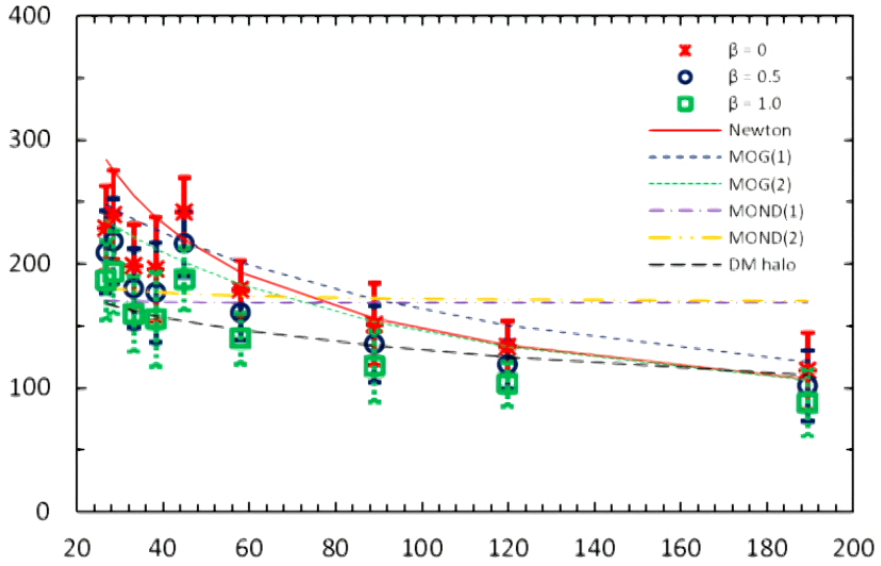

The solid red line is the Newtonian fit with a mass $M = 5 \times 10^{11} M_\odot$. The blue medium dashed and green short dashed lines correspond to MOG using the values $M = 4 \times 10^{10} M_\odot$, $\alpha = 15.01$, $\mu = 0.0313$ kpc^{-1}, and $M = 5 \times 10^{10} M_\odot$, $\alpha = 8.89$, $\mu = 0.04$ kpc^{-1}, respectively. The purple dash-dotted line is MOND with $M = 5 \times 10^{10} M_\odot$, $a_0 = 1.21 \times 10^{-8}$ cm/s^2 The black long - dashed line is the dark matter halo prediction.

17

MOG Fit To Milky Way Galaxy

JWM and V. T. Toth, Phys. Rev. D91, 043004 (2015), arXiv:1411.6701 [astro-ph.GA]

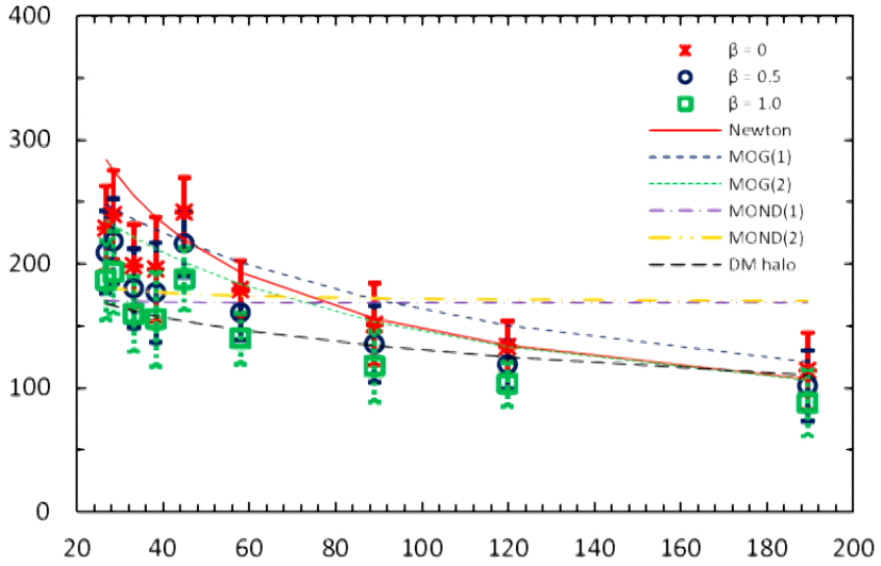

The solid red line is the Newtonian fit with a mass $M = 5 \times 10^{11} M_\odot$. The blue medium dashed and green short dashed lines correspond to MOG using the values $M = 4 \times 10^{10} M_\odot$, $\alpha = 15.01$, $\mu = 0.0313$ kpc^{-1}, and $M = 5 \times 10^{10} M_\odot$, $\alpha = 8.89$, $\mu = 0.04$ kpc^{-1}, respectively. The purple dash-dotted line is MOND with $M = 5 \times 10^{10} M_\odot$, $a_0 = 1.21 \times 10^{-8}$ cm/s^2 The black long - dashed line is the dark matter halo prediction.

We can obtain the flat rotation curves from the best fit and compare them to the observed luminosity of galaxies (Tully-Fisher relation):

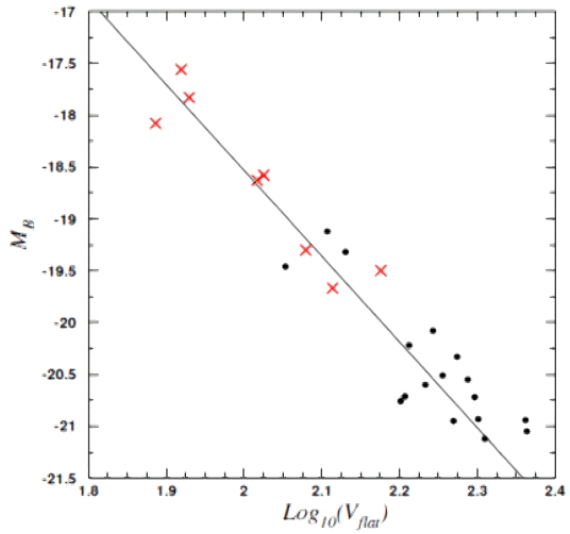

The best fit is obtained for $M = -8.27 \times \log(V_{flat}) - 1.99$

$V_{flat}^{n} \sim M_{bar}$ n=3.31

Galaxy acceleration baryon matter correlation (J. W. M, arXiv:1610.06909. S. McGaugh, F. Lelli and J. Schombert, Phys. Rev. Lett. 117, 201101 (2016)).

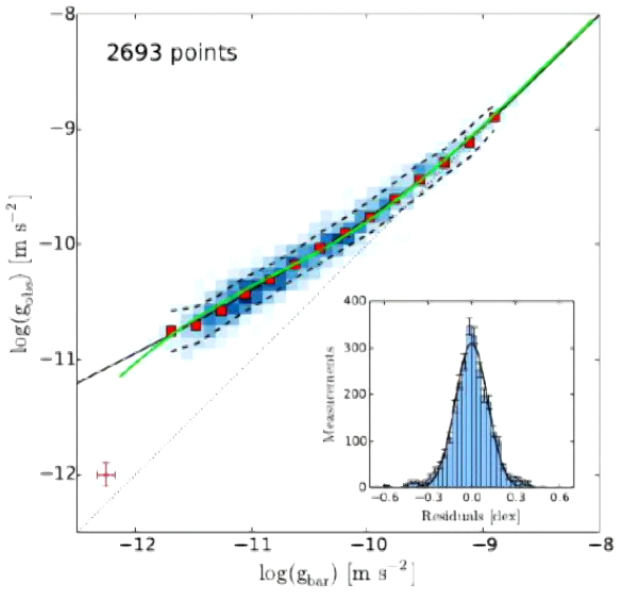

Figure 3: The centripital acceleration $g_{\rm obs}$ is plotted against that predicted by the distribution of baryons, $g_{\rm bar} = a_{\rm bar}$. The solid black curve is a fit to the empirical formula (21) and the solid green curve is the MOG prediction using $a_{\rm MOG}$.

Credit: Martin Green

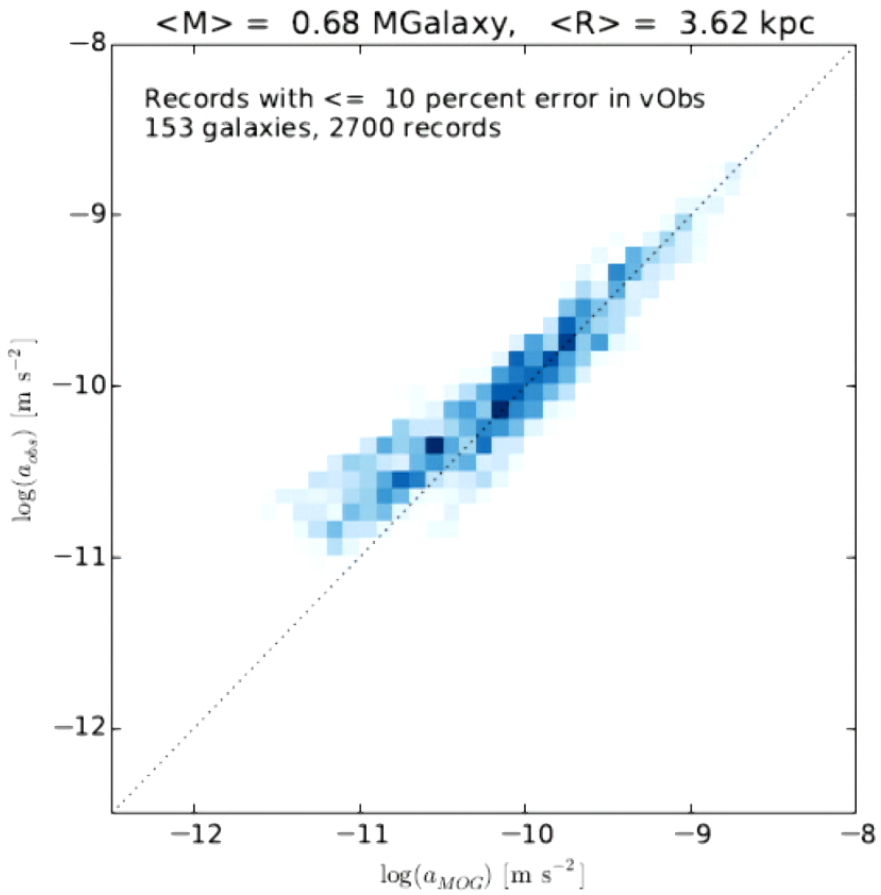

Credit: Martin Green

R. Genzel et al. Nature 543, 397 2017, arXiv:1703.04310

Strongly baryon-dominated disk galaxies at the peak of galaxy formation 10 billion years ago.

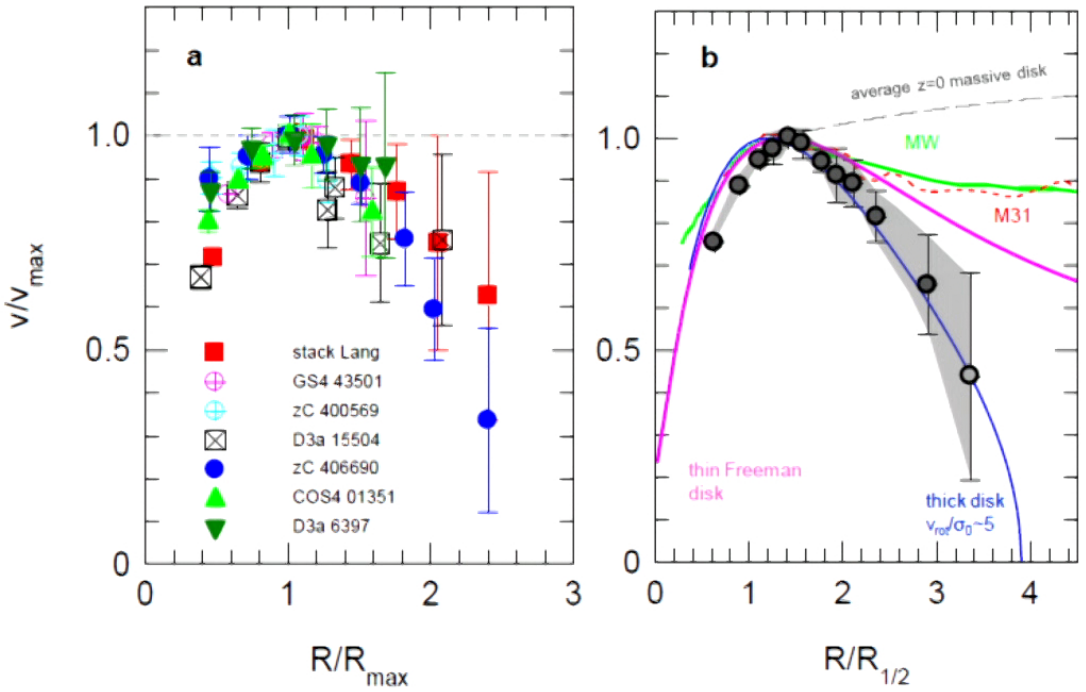

4. Cluster Dynamics (JWM & S. Rahvar, MNRAS, 441, 3724 (2014), arXiv:1309.5077 [astro-ph].

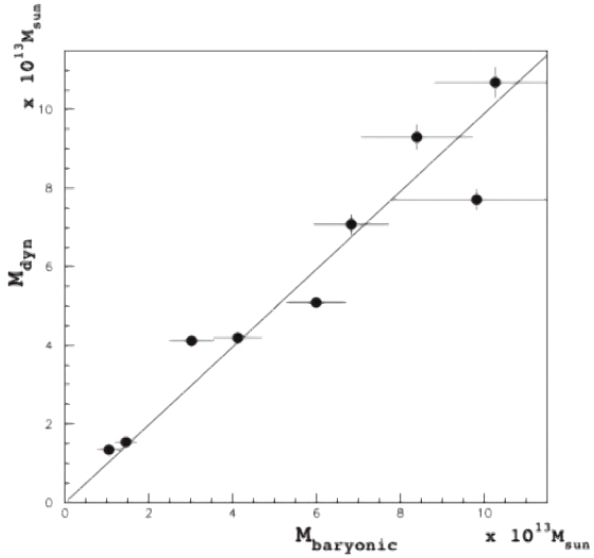

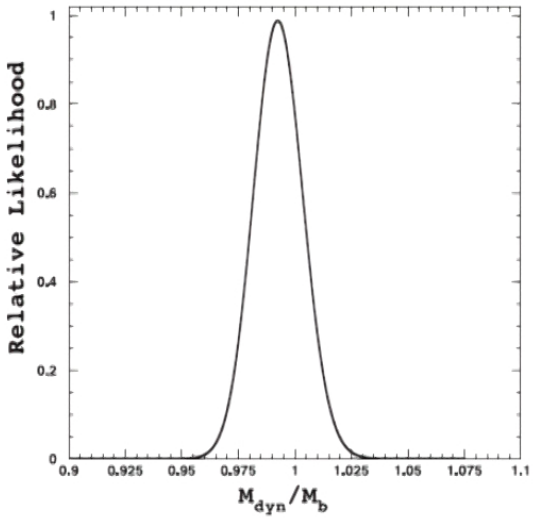

Comparison of the dynamical mass in MOG versus the baryonic mass for clusters. The baryonic mass is composed of gas and stars. The filled circles indicate the corresponding masses up to r_{500} with the corresponding error bars. The solid line shows the best fit to the linear relation $M_{\rm dyn} = \beta_{\rm cl} M_{\rm bar}$ between the two masses with the best fit value of $\beta = 0.99$. The likelihood function for this fit is given in the right-hand panel. The parameter values $\alpha = 8.89 \pm 0.34$ and $\mu = 0.042 \pm 0.004\,{\rm kpc}^{-1}$ are used to fit the cluster data.

Bullet Cluster 1E0657-558 and Abell 520 Cluster Collisions (J. R. Brownstein and JWM, MNRAS, 382, 29 (2007), arXiv:0702146 [astro-ph]. N. Israel and JWM, arXiv:1606.09128 [astro.ph]).

- The κ –convergence predicted by MOG for the weak and strong lensing by the merging clusters accounts for the off-set of mass observed for the Bullet Cluster by Clowe et al. 2006 and for Abell 520 by Jee et al. 2012 – 2014.

$$\kappa(x,y) = \int \frac{4\pi G(r)}{c^2}\frac{D_l D_{ls}}{D_s}\rho(x,y,z)dz \equiv \frac{\bar{\Sigma}(x,y)}{\Sigma_c},$$

where

$$\bar{\Sigma}(x,y) = \int \mathcal{G}(r)\rho(x,y,z)dz \quad \mathcal{G}(r) \equiv \frac{G(r)}{G_N} = 1+\sqrt{\frac{M_0}{M(r)}}\left\{1-\exp\left(-\frac{r}{r_0}\right)\left(1+\frac{r}{r_0}\right)\right\}$$

$$\alpha = \sqrt{\frac{M_0}{M(r)}} \qquad \mathcal{G}_\infty = 1+\sqrt{\frac{M_0}{M}} = 1+\alpha$$

- The baryon matter in the collisionless galaxies passes to the sides of the cluster collision. Their enhanced gravity
- ($G=G_N(1+\text{alpha})$) shifts the lensing peaks making the peaks offset from the central X-ray gas.

Abell 520 a threat to dark matter models? (Jee et al., ApJ. 747, 96 (2012) arXiv:1202.6368; ApJ. 783, 78 (2014), arXiv:1401.3356). (N. Israel and JWM, arXiv:1606.09128 [astro.ph]).)

- Data from NASA's Chandra X-ray Observatory show the hot gas in the colliding clusters colored in green. The gas provides evidence that a collision took place. Optical data from NASA's Hubble Space Telescope and the Canada-France-Hawaii Telescope (CFHT) in Hawaii are shown in red, green, and blue. Starlight from galaxies within the clusters, derived from observations by the CFHT and smoothed to show the location of most of the galaxies, is colored orange.

Abell 1689. JWM and M. H. Zhoolideh Haghighi (arXiv:1611.05382)

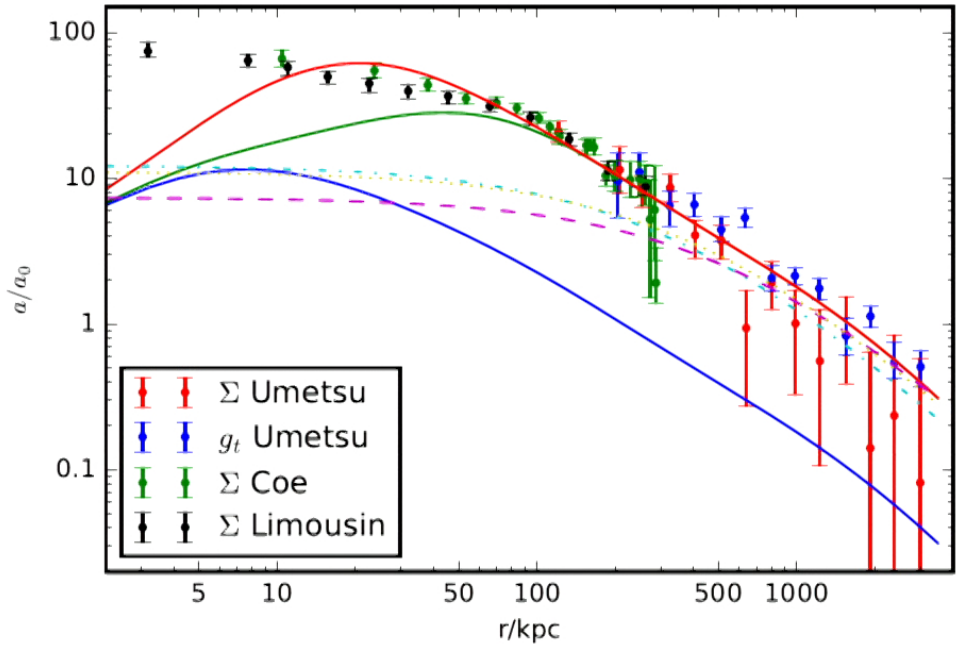

Figure 1. The full red curve is the MOG prediction for acceleration with $\alpha = 8.89$ and $\mu = 0.125\,\mathrm{kpc}^{-1}$,The full green curve is the MOG prediction for acceleration with $\alpha = 8.89$ and $\mu = 0.042\,\mathrm{kpc}^{-1}$, the dash-dotted curve is the NFW prediction with $\rho_0 = 9.6 \times 10^{-25} h^2 \mathrm{gr/cm}^3$ and $r_s = 175 \pm 18\,h^{-1}\mathrm{kpc}$ from (Lemze et al. 2008), the dashed curve is for NFW from (Broadhurst et al. 2005) with $r_s = 310^{+140}_{-120} kpc/h$ and $C_{200} = 6.5^{1.9}_{-1.6}$, the dotted curve is for NFW from (Umetsu et al. 2015) with $C_{200} = 8.9 \pm 1.1$ and $M_{200} = (1.3 \pm 0.11) \times 10^{15} M_\odot h^{-1}$ and the full blue curve is the MOND and Newtonian predictions.

5. MOG Cosmology (JWM, JCAP 0603004 (2006), arXiv:gr-qc/0506021. JWM and V. T. Toth, Galaxies, 1,65 (2013), arXiv:1104.2957 [astro-ph.CO])

The neutral pressurelss particles – the gravitational ϕ_μ vector field - can form a cold Bose-Einstein condensate fluid before decoupling and recombination (JWM, arXiv:astro-ph/0602607). We have

$$\rho = \rho_m + \rho_r + \rho_d, \quad \rho_m = \rho_b + \rho_\phi + \rho_G + \rho_\mu, \quad \rho_r = \rho_\gamma + \rho_\nu$$

- We assume that ρ_ϕ dominates in the early universe, before the formation of stars and galaxies and $G \sim G_\infty \sim G_N$

- At the formation of stars and galaxies and reionization $\rho_b > \rho_\phi$

$$(G_N\rho)_{\Lambda CDM} = (G_N(1+\alpha)\rho)_{\rm MOG}, \quad \rho_{\Lambda CDM} = \rho_b + \rho_{CDM} \qquad \rho_{\rm MOG} = \rho_b$$

Structure growth for baryon-only matter and the gravitational, neutral vector particle fluid.

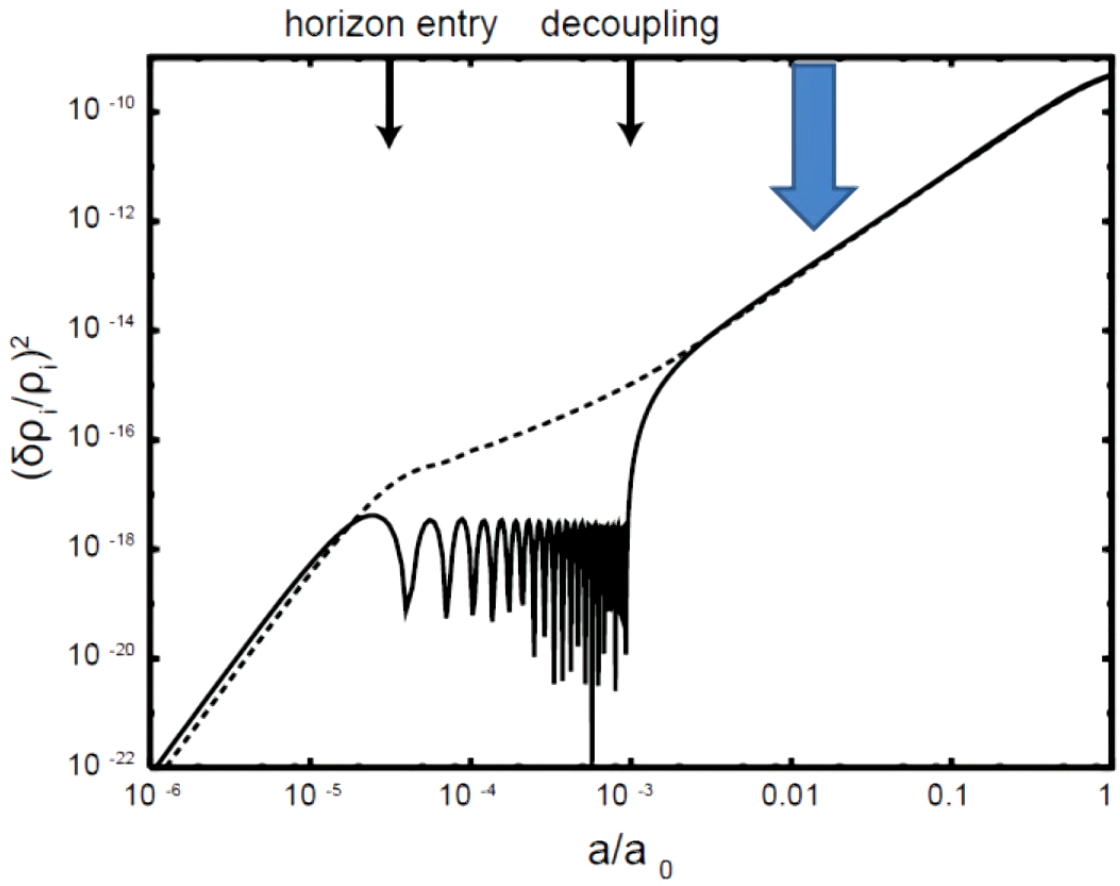

Jeans equation for structure growth:

$$\ddot{\delta}_{\mathbf{k}} + 2H\dot{\delta}_{\mathbf{k}} - 4\pi G_N \bar{\rho}\delta_{\mathbf{k}} = 0,$$

Jeans length:

$$k_J^{-1} = \frac{a_0 c_s}{a\sqrt{4\pi G_N \bar{\rho}}}$$

At the CMB decoupling:

$\Delta T/T \sim 10^{-4} \sim \delta\rho_b$

The CMB angular TT power spectrum with $\rho_\phi > \rho_b$

$$\Omega_m = \Omega_b + \Omega_\phi \qquad \Omega_b h^2 = 0.022199, \quad \Omega_\Lambda = 0.6939, \qquad \sigma_8 = 0.8271$$

$$\Omega_c h^2 = 0.11847, \; n_s = 0.9624, \; H_0 = 67.94\,\mathrm{km\,sec^{-1}\,Mpc^{-1}}$$

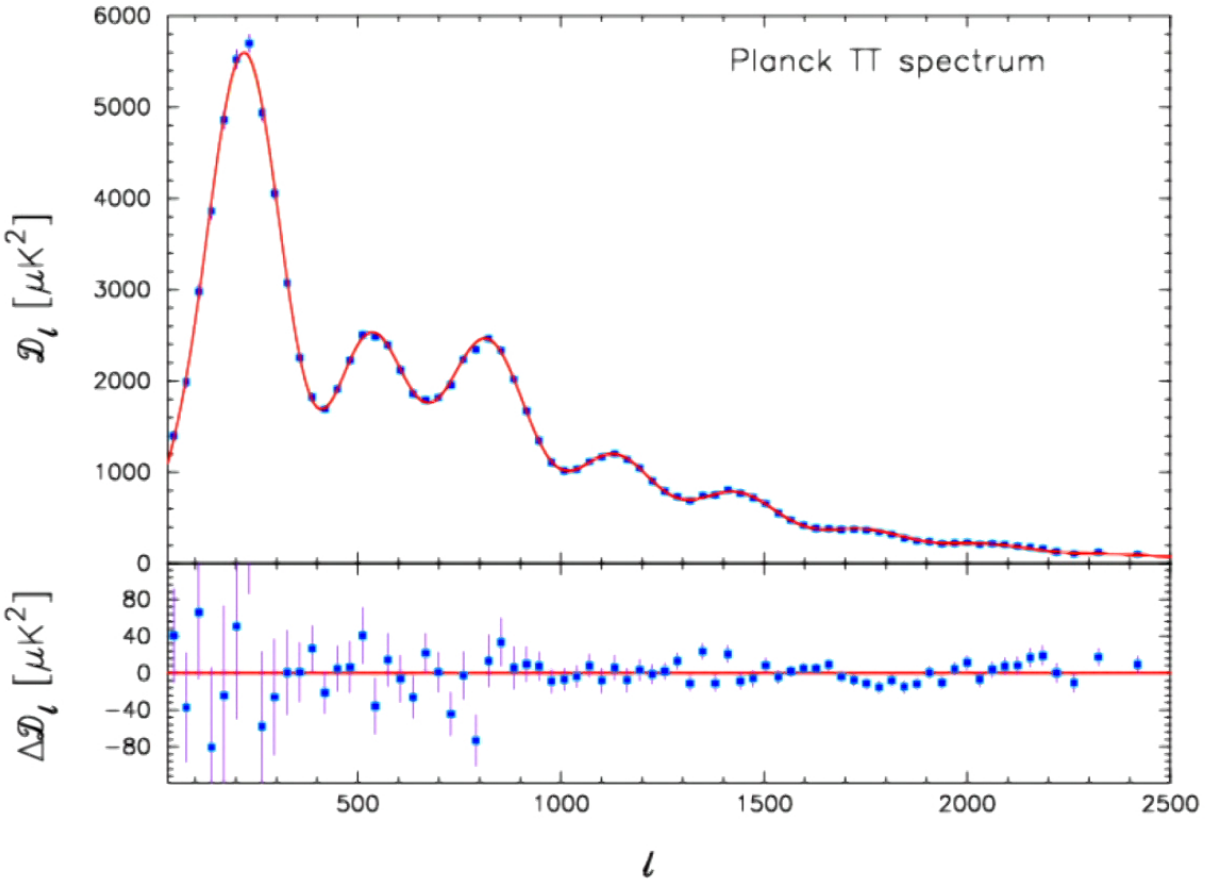

Matter Power Spectrum (J. W. Moffat and V. T. Toth, Galaxies, 1, 65 (2013), arXiv:1104.2957 [astro-ph.CO].)

Figure 1. The matter power spectrum. Three models are compared against five data sets (see text): Λ-cold dark matter (Λ-CDM) (dashed blue line, $\Omega_b = 0.035$, $\Omega_c = 0.245$,$\Omega_\Lambda = 0.72$, $H = 71$ km/s/Mpc), a baryon-only model (dotted green line, $\Omega_b = 0.035$, $H = 71$ km/s/Mpc) and modified gravity (MOG) (solid red line, $\alpha = 19$, $\mu = 5$ h Mpc^{-1}, $\Omega_b = 0.035$, $H = 71$ km/s/Mpc). Data points are colored light blue [Sloan Digital Sky Survey (SDSS) 2006], gold (SDSS 2004), pink [Two-degree-Field (2dF)], light green [UK Schmidt Telescope (UKST)] and dark blue (CfA).

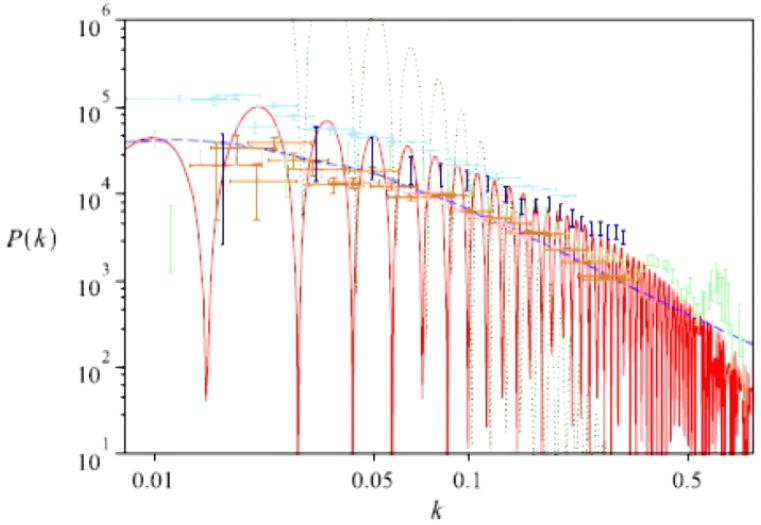

- In the present universe z = 0 and

$$G = G_N(1+\alpha) \qquad \Omega_m = \Omega_b(1+\alpha)$$

- The matter power spectrum determined by the distribution of matter obtained from large scale galaxy surveys can also be predicted by MOG. A suitable window function and an initial scale invariant power spectrum P_0 are chosen to determine P(k). Baryon unit oscillations are greatly dampened by the window function.

$$(G_N\rho)_{\Lambda CDM} = (G_N(1+\alpha)\rho)_{\rm MOG} \qquad \rho_{\Lambda CDM} = \rho_b + \rho_{CDM} \qquad \rho_{\rm MOG} = \rho_b$$

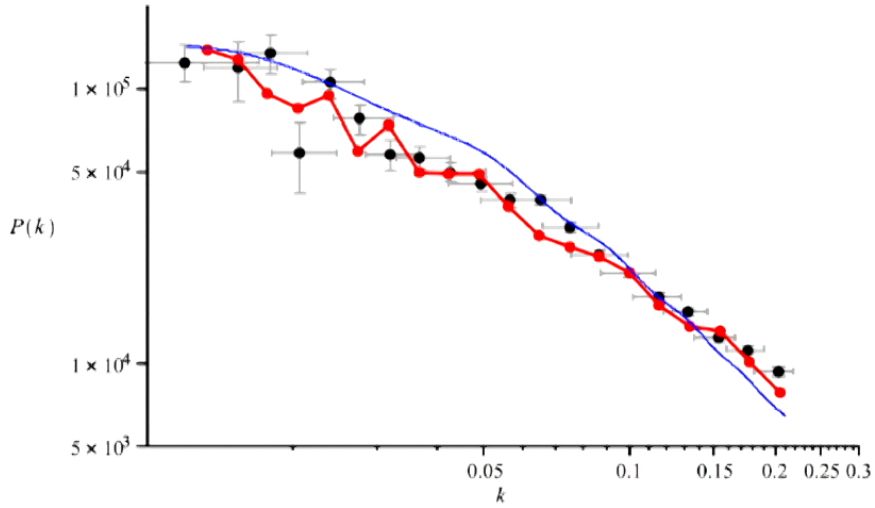

- With large scale surveys of galaxies, unit baryon oscillations will be observable to distinguish MOG from ΛCDM.

6. MOG Black Holes

JWM, Eur. Phys. J. C (2015) 75, 175, arXiv:1412.5424 [gr-qc] and JWM, Eur. Phys. J. C (2015) 75, 130, arXiv:1502.01677 [gr-qc]. J. R. Mureika, JWM and Mir Faizal, Phys. Lett. B757, 528 (2016), arXiv:1504.08226 [gr-qc]. JWM, Phys. Lett. B 763, 427 (2016), arXiv:1603.05225.

- The gravi-ϕ_μ vacuum STVG field equations are ($T_{M\mu\nu}=0$) :

$$R_{\mu\nu} = -8\pi G T_{\phi\mu\nu}$$

- We choose $\partial_\nu G \sim 0$ and we ignore the small vector field mass $m_\phi = 2.6 \times 10^{-28}$ eV ($\mu^{-1} = 24\,\mathrm{kpc}$) for compact-sized bodies. The field equations are

$$T_{\phi\mu\nu} = -\frac{1}{4\pi}(B_\mu{}^\alpha B_{\nu\alpha} - \frac{1}{4} g_{\mu\nu} B^{\alpha\beta} B_{\alpha\beta}) \qquad B_{\mu\nu} = \partial_\mu \phi_\nu - \partial_\nu \phi_\mu$$

$$\nabla_\nu B^{\mu\nu} = \frac{1}{\sqrt{-g}} \partial_\nu (\sqrt{-g} B^{\mu\nu}) = 0 \quad \partial_\sigma B_{\mu\nu} + \partial_\mu B_{\nu\sigma} + \partial_\nu B_{\sigma\mu} = 0$$

- The Schwarzschild-MOG and Kerr-MOG black hole metrics are

$$ds^2 = \left(1 - \frac{2G_N(1+\alpha)M}{r} + \frac{G_N^2\alpha(1+\alpha)M^2}{r^2}\right)dt^2 - \left(1 - \frac{2G_N(1+\alpha)M}{r} + \frac{G_N^2\alpha(1+\alpha)M^2}{r^2}\right)^{-1} dr^2 - r^2 d\Omega^2$$

$$ds^2 = \left(1 - \frac{r_s r - r_Q^2}{\rho^2}\right)dt^2 - \left[r^2 + a^2 + a^2\sin^2\theta\left(\frac{r_g r - r_Q^2}{\rho^2}\right)\right]\sin^2\theta d\phi^2$$

$$+2\sin^2\theta\left(\frac{r_g r - r_Q^2}{\rho^2}\right)dt d\phi - \frac{\rho^2}{\Delta}dr^2 - \rho^2 d\theta^2,$$

$$\rho^2 = r^2 + a^2\cos^2\theta \qquad \Delta = r^2 - r_g r + a^2 + r_Q^2$$

- Horizons are determined by

$$r_\pm = G_N M\left(1 + \alpha \pm \sqrt{1+\alpha}\right) \qquad r_\pm = G_N(1+\alpha)M\left[1 \pm \sqrt{1 - \frac{a^2}{G_N^2(1+\alpha)^2M^2} - \frac{\alpha}{1+\alpha}}\right]$$

$$r_s = 2G_N(1+\alpha)M,\ a = J/M\ r_Q^2 = G_N^2\alpha(1+\alpha)M^2$$

Black Hole Shadows (Silhouettes) (JWM, Eur. Phys. J. C (2015) 75, 130, arXiv:1502.01677 [gr-qc]; T. Johannsen et al. Phys. Rev. Lett. 116 031101 (2016), arXiv:1512.02640 [astro-ph.GA])

We shall take it as given that our modified gravity–Schwarzschild and modified gravity–Kerr black holes are characterized by only the two parameters mass M and angular momentum J. They are stationary and asymptotically flat solutions and they satisfy the "no-hair" theorem. An interesting consequence of these properties of the solution is that the shadow outline created by the black hole is determined by M and $a = J/M$ and the relative position of an asymptotic observer.

- The black hole casts a shadow in front of an illuminated background in the asymptotically flat region and the shadow is determined by a set of closed photon orbits.

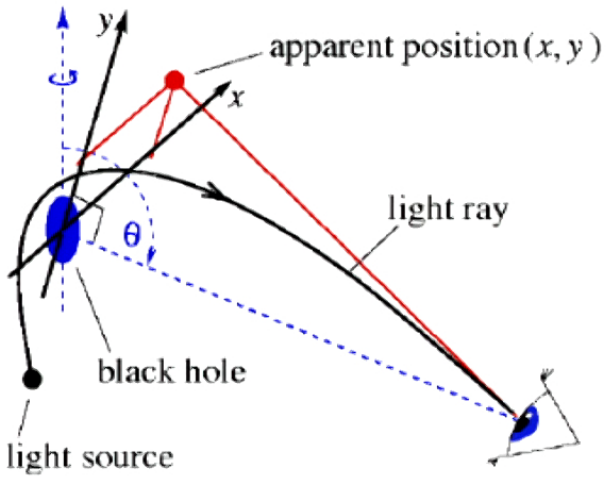

Figure 1: The apparent position of a light ray with respect to the observer's projection plane in the x,y coordinates containing the center of the spacetime: x denotes the apparent distance from the rotation axis, and y the projection of the rotation axis itself (dashed line). The angle θ denotes the angle of latitude, reaching from the north pole at $\theta = 0$ to the south pole at $\theta = \pi$ (image by de Vries).

- The shadow radius for the Schwarzschild-MOG black hole is

$$r_{\rm shad} = \frac{\left[3(1+\alpha) \pm \sqrt{(9+\alpha)(1+\alpha)}\right]^2}{\left\{4\left[(1+\alpha) \pm \sqrt{(9+\alpha)(1+\alpha)}\right]^2 - 16(1+\alpha)\right\}^{1/2}} G_N M$$

- The shadow radius can be approximated by

$$r_{\rm shad} \sim (2.59 + 2\alpha) r_s$$

- The angular radius is given by $R = (5.19 + 4\alpha) r_g$ /D where D=8.3 kpc and $r_g = G_N M/c^2$. For α =0 and M = 4.23X 10^6 M_{SUN} we get

$$R = 26\,\mu as$$

For α = 1 we get

$$R = 46\,\mu as$$

- The Event Horizon Telescope observations should be able to determine the size and shape of the black hole shadow to 5 to 10 % accuracy, provided that the effect of the accretion disk surrounding the black hole can be determined. Successful observations can distinguish between strong gravity MOG black holes ($\alpha > 0$) and GR black holes ($\alpha = 0$).

7. MOG AND GRAVITATIONAL WAVES

- We expand the metric about Minkowski spacetime:

$$g_{\mu\nu} = \eta_{\mu\nu} + \lambda h_{\mu\nu} \qquad \gamma^{\mu\nu} = h^{\mu\nu} - \frac{1}{2}\eta^{\mu\nu}h$$

$$\Box\gamma^{\mu\nu} = -\lambda T^{M\mu\nu} \qquad \gamma^{\mu\nu}(\mathbf{x},t) = -\frac{\lambda}{4\pi}\int d^3x' \frac{T^{M\mu\nu}(t-|\mathbf{x}-\mathbf{x}'|,\mathbf{x}')}{|\mathbf{x}-\mathbf{x}'|}$$

$$\frac{1}{G}\Box G = \frac{8\pi G}{3+16\pi}T^M \qquad \Box\mu = 0. \qquad \partial_\nu T^{M\mu\nu} = 0.$$

- The total power of gravitational wave energy is

$$P = \frac{\mathcal{G}}{45c^5}\dddot{Q}_{kl}\dddot{Q}_{kl} \qquad Q_{kl} = \int d^3x' \left(3x'_k x'_l - r'^2\delta_{kl}\right)\rho_M(\mathbf{x}')$$

$$a(r) = -\frac{\mathcal{G}(r)M}{r^2} \qquad \mathcal{G}(r) = G_N[1+\alpha-\alpha\exp(-\mu r)(1+\mu r)]$$

- During the merging of the black holes in the last ~ 0.2 sec and the final ringdown phase, the MOG gravitational charges Q_1 and Q_2 and spins S_1 and S_2 coalesce to produce the final quiescent MOG black hole.

$$h_+(t) \sim \frac{G_N^2(1+\alpha)^2 m_1 m_2}{DR(t)c^4}(1+\cos^2\,\iota)\cos\left(\int^t f(t')dt'\right),$$

$$\mathcal{M}_c = \frac{(m_1 m_2)^{3/5}}{(m_1+m_2)^{1/5}} = \frac{c^3}{G_N(1+\alpha)}\left[\frac{5}{96}\pi^{-8/3} f^{-11/3}\dot{f}\right]^{3/5},$$

$$\dot{f} = \frac{96}{5}\frac{c^3 f}{G_N(1+\alpha)\mathcal{M}_c}\left(\frac{\pi f}{c^3}G_N(1+\alpha)\mathcal{M}_c\right)^{8/3}.$$

$$\alpha = \frac{\mathcal{M}_{c\mathrm{GR}} - \mathcal{M}_{c\mathrm{MOG}}}{\mathcal{M}_{c\mathrm{MOG}}}$$

LIGO Observed Gravitational Wave GW150914

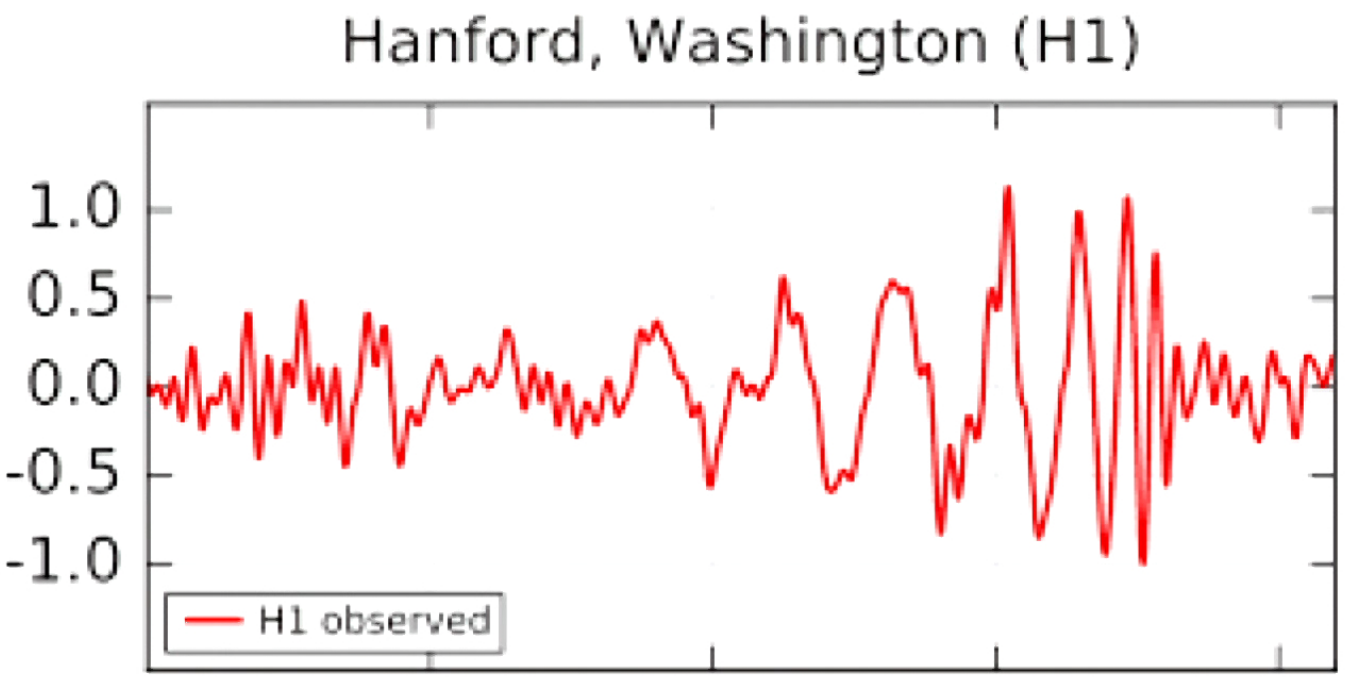

- Since G=G_N(1+alpha) always multiplies M, then for alpha > 1, m_1 and m_2 are smaller than GR to give a fit to the LIGO GW 150914 and GW 151226 GW detection events.

Merging systems	α	$m_1(M_\odot)$	$m_2(M_\odot)$	$\mathcal{M}_c(M_\odot)$
GR GW150914	0	36	29	28
GR GW151226	0	14	8	8.9
MOG GW150914	2.6	10	8	7.8
MOG GW151226	2.0	4.7	3	3
MOG GW150914	5.7	6	4	4.2
MOG GW150914	8.3	4	3	3

- The effective spin parameter is:

$$\chi_{\rm eff} = \frac{c}{GM}\left(\frac{\mathbf{S}_1}{m_1} + \frac{\mathbf{S}_2}{m_2}\right)\cdot\hat{\mathbf{L}} = \frac{m_1\mathbf{a}_1 + m_2\mathbf{a}_2}{m_1+m_2}\cdot\hat{\mathbf{L}}$$

The observed value is $\chi_{\rm eff} = -0.06^{+0.17\pm0.01}_{-0.18\pm0.07}$ For alpha > 1 the predicted value of $\chi_{\rm eff}$ for GW150914 in MOG can be made to agree with the observed value and stellar black hole evolution models.

8. Conclusions

- It has been demonstrated that MOG can fit available observational data for the solar system to galaxy, galaxy clusters and structure growth (matter power spectrum) without exotic dark matter. The CMB cosmological data can be fitted with a gravitational vector field density fluid with a small vector field mass $m_\phi >\sim 10^{-22}$ eV and baryon matter fluid

- The EHT and LIGO gravitational observations will test the predictions for MOG black holes.

- The EHT observation of the size of the Sagittarius A* shadow, expected to be available in 2017 -18, will be an interesting test of the gravity theory.